Tracing the source of nitrate in a forested stream showing elevated concentrations during storm events

Weitian Ding[1], Urumu Tsunogai[1], Fumiko Nakagawa[1], Takashi Sambuichi[1], Hiroyuki Sase[2], Masayuki Morohashi[2], Hiroki Yotsuyanagi[2]

[1] Graduate School of Environmental Studies, Nagoya University, Furo-cho, Chikusa-ku, Nagoya 464-8601, Japan

[2]Asia Center for Air Pollution Research, 1182 Sowa, Nishi-ku, Niigata-shi, Niigata 950-2144, Japan

Corresponding author: Weitian Ding, Email: ding.weitian.v2@s.mail.nagoya-u.ac.jp

Abstract

To clarify the source of nitrate increased during storm events in a temperate forested stream, we monitored temporal variation in the concentrations and stable isotopic compositions including $\Delta^{17}O$ of stream nitrate in a forested catchment (KJ catchment, Japan) during three storm events I, II, and III (summer). The stream showed significant increase in nitrate concentration, from 24.7 μM to 122.6 μM, from 28.7 μM to 134.1 μM, and from 46.6 μM to 114.5 μM during the storm events I, II, and III, respectively. On the other hand, the isotopic compositions ($\delta^{15}N$, $\delta^{18}O$, and $\Delta^{17}O$) of stream nitrate showed a decrease in accordance with the increase in the stream nitrate concentration, from +2.5 ‰ to −0.1 ‰, from +3.0 ‰ to −0.5 ‰, and from +3.5 ‰ to −0.1 ‰ for $\delta^{15}N$, from +3.1 ‰ to −3.4 ‰, from +2.9 ‰ to −2.5 ‰, and from +2.1 ‰ to −2.3 ‰ for $\delta^{18}O$, and from +1.6 ‰ to +0.3 ‰, from +1.4 ‰ to +0.3 ‰, and from +1.2 ‰ to +0.5 ‰ for $\Delta^{17}O$ during the storm events I, II, and III, respectively. Besides, we found strong linear relationships between the isotopic compositions of stream nitrate and the reciprocal of stream nitrate concentrations during each storm event, implying that the temporal variation in the stream nitrate can be explained by simple mixing between two distinctive endmembers of nitrate having different isotopic compositions. Furthermore, we found that both concentrations and the isotopic compositions of soil nitrate obtained in the riparian zone of the stream were plotted on the nitrate-enriched extension of the linear relationship. We conclude that the soil nitrate in the riparian zone was primarily responsible for the increase in stream nitrate during the storm events. In addition, we

found that the concentration of unprocessed atmospheric nitrate in the stream was stable at 1.6 ± 0.4 μM, 1.8 ± 0.4 μM, and 2.1 ± 0.4 μM during the storm events I, II, and III, respectively, irrespective to the significant variations in the total nitrate concentration. We conclude that the storm events have little impacts on the concentration of unprocessed atmospheric nitrate in the stream and thus the annual export flux of unprocessed atmospheric nitrate relative to the annual deposition flux can be a robust index to evaluate nitrogen saturation in forested catchments, irrespective to the variation in the number of storm events and/or the variation in the elapsed time from storm events to sampling.

1 Introduction

Nitrate is an important nitrogenous nutrient in biosphere. Traditionally, forested ecosystems have been considered nitrogen limited (Vitousek and Howarth, 1991). Due to the elevated loading of nitrogen through atmospheric deposition, however, some forested ecosystems become nitrogen saturated (Aber et al., 1989), from which elevated levels of nitrate are exported (Mitchell et al., 1997; Peterjohn et al., 1996). In addition, sudden increase in the concentration of nitrate in response to storm events has been reported in forested streams worldwide (Aguilera and Melack, 2018; Creed et al., 1996; Kamisako et al., 2008; McHale et al., 2002), which further enhanced nitrate export from forested ecosystems.

Such excessive leaching of nitrate from forested catchment degrades water quality

and cause eutrophication in downstream areas (Galloway et al., 2003; Paerl and Huisman, 2009). Thus, tracing the source of nitrate increase during storm events in forested streams is important for sustainable forest management, especially for the nitrogen-saturated forested ecosystems.

As for the source of nitrate that was added to stream during storm events, either of the two possible sources have been assumed in past studies; (1) atmospheric nitrate ($NO_3^-{}_{atm}$) in rainwater originally and being supplied directly to stream water (Inamdar and Mitchell, 2006), and (2) soil nitrate originally and being supplied to stream water by the flushing effects on soils (Creed et al., 1996; Ocampo et al., 2006). Nevertheless, monitoring the variation in nitrate concentration, it is difficult to clarify the primary source of nitrate that increases during storm events.

The natural stable isotopic composition of nitrate has been widely applied to clarify the sources of nitrate in natural freshwater systems (Burns and Kendall, 2002; Durka et al., 1994; Kendall et al., 2007). In particular, triple oxygen isotopic compositions of nitrate ($\Delta^{17}O$) have been used in recent days as a conservative tracer of $NO_3^-{}_{atm}$ deposited onto a forested catchment (Inoue et al., 2021; Michalski et al., 2004; Nakagawa et al., 2018; Tsunogai et al., 2014), showing distinctively different $\Delta^{17}O$ from that of remineralized nitrate ($NO_3^-{}_{re}$), derived from organic nitrogen through general chemical reactions, including microbial N mineralization and microbial nitrification. While $NO_3^-{}_{re}$, the oxygen atoms of which are derived from either terrestrial O_2 or H_2O through microbial processing (i.e., nitrification), always shows the relation close to the

64 "mass-dependent" relative relation between $^{17}O/^{16}O$ ratios and $^{18}O/^{16}O$ ratios; $NO_3^-{}_{atm}$
65 displays an anomalous enrichment in ^{17}O reflecting oxygen atom transfers from
66 atmospheric ozone (O_3) during the conversion of NO_X to $NO_3^-{}_{atm}$ (Alexander et al.,
67 2009; Michalski et al., 2003; Morin et al., 2011; Nelson et al., 2018). As a result, the
68 $\Delta^{17}O$ signature defined by the following equation (Kaiser et al., 2007) enables us to
69 distinguish $NO_3^-{}_{atm}$ ($\Delta^{17}O > 0$) from $NO_3^-{}_{re}$ ($\Delta^{17}O = 0$):

70 $$\Delta^{17}O = \frac{1+\delta^{17}O}{(1+\delta^{18}O)^{\beta}} - 1 \quad (1)$$

71 where the constant β is 0.5279 (Kaiser et al., 2007), $\delta^{18}O = R_{sample}/R_{standard} - 1$ and R is
72 the $^{18}O/^{16}O$ ratio (or the $^{17}O/^{16}O$ ratio in the case of $\delta^{17}O$ or the $^{15}N/^{14}N$ ratio in the case
73 of $\delta^{15}N$) of the sample and each standard reference material. In addition, $\Delta^{17}O$ is almost
74 stable during "mass-dependent" isotope fractionation processes within terrestrial
75 ecosystems. Therefore, while the $\delta^{15}N$ or $\delta^{18}O$ signature of $NO_3^-{}_{atm}$ can be overprinted
76 by the biological processes subsequent to deposition, $\Delta^{17}O$ can be used as a robust tracer
77 of unprocessed $NO_3^-{}_{atm}$ to reflect its accurate mole fraction within total NO_3^-, regardless
78 of the progress of the partial metabolism (partial removal of nitrate through
79 denitrification and assimilation) subsequent to deposition (Michalski et al., 2004;
80 Nakagawa et al., 2013, 2018; Tsunogai et al., 2011, 2014, 2018).

81 While the variation in the $\delta^{18}O$ and/or $\Delta^{17}O$ of nitrate in forested streams during storm
82 events have been reported in past studies (Sebestyen et al., 2019; Sabo et al., 2016;
83 Buda and Dewalle. 2009), the temporal resolutions of sampling were less than 10
84 times/day during storm events and the source of the stream nitrate increased during

85 storm events has not been clarified yet. In this study, we determined the temporal
86 variation in the concentrations and the isotopic compositions ($\delta^{15}N$, $\delta^{18}O$, and $\Delta^{17}O$) of
87 stream nitrate at once every hour during storm events in a forested catchment to clarify
88 (1) the source of nitrate in a forested stream that was added during storm events, and
89 (2) the temporal variation in the concentration of $NO_3^-{}_{atm}$ in response to storm events.
90 In addition, the impacts of storm events on the index of nitrogen saturation lately
91 proposed by Nakagawa et al. (2018) were discussed.
92
93 **2 Methods**
94 2.1 Study site
95 As for the studying field to trace the source of stream nitrate during storm events, we
96 chose Kajikawa forested catchment (KJ catchment) in Japan, in which several past
97 studies had been done to clarify the temporal variation in the concentration of stream
98 nitrate and the status of nitrogen saturation (Kamisako et al., 2008; Nakagawa et al.,
99 2018; Sase et al., 2021). This is a small, forested catchment (3.84 ha) located in the
100 northern part of Shibata City, Niigata Prefecture, along the coast of Sea of Japan (Fig.
101 1a). The KJ catchment predominantly slopes towards the west-northwest, with a mean
102 slope of 36°, and the elevation ranges from 60 to 170 m above sea level (Fig. 1b). The
103 catchment is fully covered by Japanese cedars (*Cryptomeria japonica* D. Don) that were
104 approximately 46 years old in 2018 (Sase et al., 2021). The parent material is
105 granodiorite and brown forest soils (Cambisols) have developed in this area (Kamisako

et al., 2008; Sase et al., 2008). The lowest, highest, and mean monthly temperatures recorded at the nearest meteorological station (Nakajo station) were 1.0 ˚C (in February), 27.9 ˚C (in August), and 14.5 ˚C, respectively, from 2017/5 to 2020/3. The annual mean precipitation was around 2500 mm, approximately 17% of which occurred during spring (from March to May), approximately 20% during summer (from June to August), approximately 28% during fall (from September to November), and approximately 35% during winter (from December to February). The catchment usually experiences snowfall from late December to March.

From 2003 to 2005, Kamisako et al. (2008) determined temporal variation in the concentration of Ca^{2+}, Mg^{2+}, Cl^{-}, and NO_3^{-} eluted from the catchment via a stream at intervals of 1 to 3 hour for 2 to 3 days on each and found that significant increase in the stream nitrate concentration during storm events, from less than 30 μM to more than 120 μM. On the basis of the observed nitrate enrichment in the stream water, they concluded that atmospheric nitrogen inputs exceeded the biological demand at the catchment and proposed that the KJ catchment was under nitrogen saturation. Nakagawa et al. (2018) determined temporal variation in the concentrations and stable isotopic compositions ($\delta^{15}N$, $\delta^{18}O$, and $\Delta^{17}O$) of both stream nitrate and soil nitrate for two years (from 2012/12 to 2014/12) and concluded that nitrate in the groundwater of the catchment was the major source of nitrate in the stream water during the base flow periods. Additionally, Nakagawa et al. (2018), who proposed the export flux of $NO_3^{-}{}_{atm}$ (M_{atm}) relative to the deposition flux of $NO_3^{-}{}_{atm}$ (D_{atm}) can be an alternative, more robust

index for nitrogen saturation in temperate forested catchments, clarified that the M_{atm}/D_{atm} ratio in the KJ catchment was larger (9.4 %) than the other catchments they studied simultaneously (6.5 % and 2.6 %), which also implied the KJ catchment was under the nitrogen saturation. Moreover, Sase et al. (2021) reported the nitrate concentration of the stream has been increasing in recent years, which implies that nitrogen saturation is still ongoing in the forest.

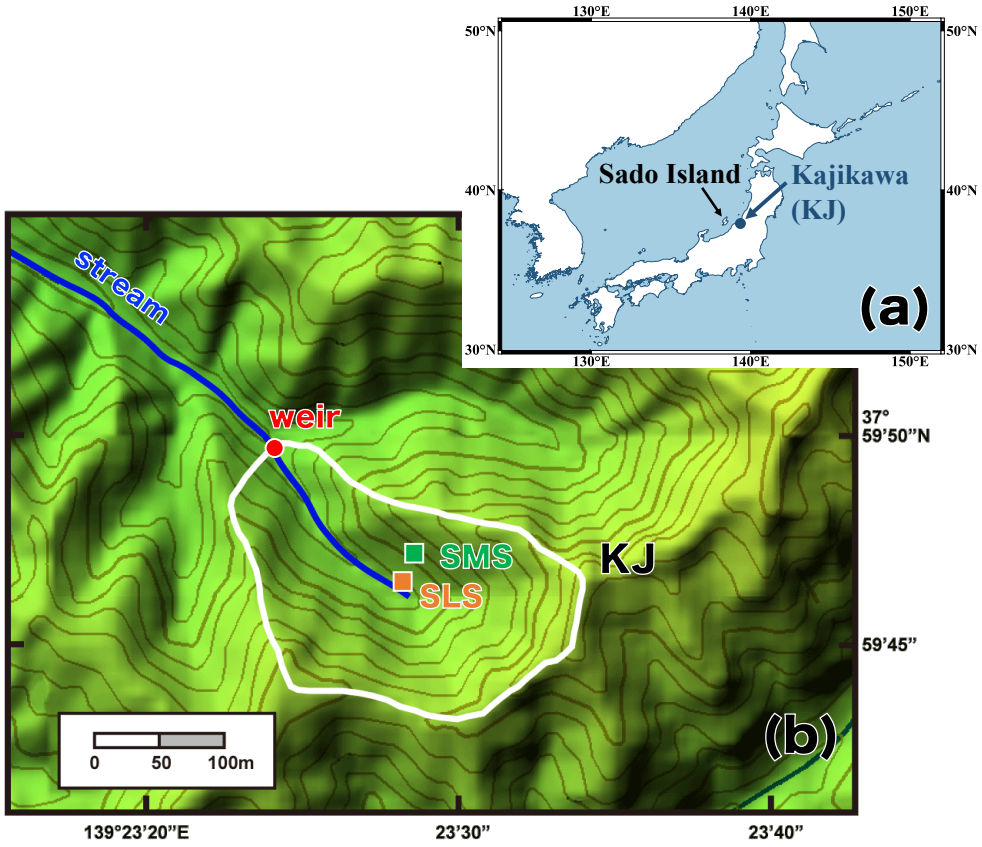

Figure 1. A map showing the locations of the studied Kajikawa (KJ) catchment in Japan (a) and a colored altitude map of the KJ catchment (b) (modified after Nakagawa et al. 2018). The white line denotes the whole catchment area, and the red circle denotes the position of the weir where the stream water was sampled. The orange (SLS) and green (SMS) squares denote the sampling stations of soil water in the riparian and upland

zone, respectively, in the past study (Nakagawa et al., 2018).

2.2 Discharge rates and weather information

A V-notch weir (half angle: 30°) and a partial flume were installed at the bottom of the catchment (Fig. 1b), where the discharge rates were determined. The weather information including the precipitation monitored by Japan Meteorological Agency at the nearest station of KJ catchment (Nakajo station; 38°04'60" N, 139°23'30" E) was used for that in the KJ catchment. Because the accumulated snow was not monitored in Nakajo station, however, those monitored at the Niigata station (37°53'60" N, 139°01'10" E) was used instead.

2.3 Sampling

In this study, the concentrations and stable isotopic compositions ($\delta^{15}N$, $\delta^{18}O$, and $\Delta^{17}O$) of stream nitrate eluted from the KJ catchment were monitored every month for more than 2 years (routine observation). Additionally, during storm events, the same parameters were monitored every hour for 1 day (intensive observation). Stream water was sampled at the weir located on the outlet of the KJ catchment (Fig. 1b). Routine observation was performed manually using bottles at the weir approximately once a month from 2017/5 to 2020/3. Intensive observation was conducted during the three storm events I, II, and III (2019/8/22, 2019/10/12, and 2020/9/13, respectively), where the water samples were collected at intervals of 1 hour over 24 hours using an automatic

160 water sampler (SIGMA 900, Hach, USA). In this study, 0.5 or 2 L polyethylene bottles
161 washed using chemical detergents were rinsed at least three times using deionized water
162 and dried in the laboratory before being used to store the water samples.
163
164 2.4 Analysis
165 Samples of stream water for the routine observation were transported to the
166 laboratory within 1 hour after being collected manually. Samples for the intensive
167 observation were transported within 12 days after completion of the automatic sampling
168 (Table 1). All samples were passed through a membrane filter (pore size 0.45 μm) and
169 stored in a refrigerator (4°C) until their chemical analysis.
170 The concentrations of nitrate were measured by ion chromatography (DX-500;
171 Dionex Inc., USA). To determine the stable isotopic compositions of nitrate in the
172 stream water samples, nitrate in each sample was chemically converted to N_2O using a
173 method originally developed to determine the $^{15}N/^{14}N$ and $^{18}O/^{16}O$ ratios of seawater
174 and freshwater nitrate (McIlvin and Altabet, 2005) that was later modified (Konno et
175 al., 2010; Tsunogai et al., 2011; Yamazaki et al., 2011). In brief, 11 mL of each sample
176 solution was pipetted into a vial with a septum cap. Then, 0.5 g of spongy cadmium
177 was added, followed by 150 μL of a 1 M $NaHCO_3$ solution. The sample was then shaken
178 for 18-24 h at a rate of 2 cycles s^{-1}. Then, the sample solution (10 mL) was decanted
179 into a different vial with a septum cap. After purging the solution using high-purity
180 helium, 0.4 mL of an azide–acetic acid buffer, which had also been purged using high-

purity helium, was added. After 45 min, the solution was alkalinized by adding 0.2 mL of 6 M NaOH.

Then, the stable isotopic compositions ($\delta^{15}N$, $\delta^{18}O$, and $\Delta^{17}O$) of the N_2O in each vial were determined using the continuous-flow isotope ratio mass spectrometry (CF-IRMS) system at Nagoya University. The analytical procedures performed using the CF-IRMS system were the same as those detailed in previous studies (Hirota et al., 2010; Komatsu et al., 2008). The obtained values of $\delta^{15}N$, $\delta^{18}O$, and $\Delta^{17}O$ for the N_2O derived from the nitrate in each sample were compared with those derived from our local laboratory nitrate standards to calibrate the values of the sample nitrate to an international scale and to correct for both isotope fractionation during the chemical conversion to N_2O and the progress of oxygen isotope exchange between the nitrate derived reaction intermediate and water (ca. 20 %). The local laboratory nitrate standards used for the calibration had been calibrated using the internationally distributed isotope reference materials (USGS-34 and USGS-35). In this study, we adopted the internal standard method (Nakagawa et al., 2013, 2018; Tsunogai et al., 2014) to calibrate the stable isotopic compositions of sample nitrate. In order to calibrate the differences in $\delta^{18}O$ of H_2O between the samples and those our local laboratory nitrate standards were added for calibration, the $\delta^{18}O$ values of H_2O in the samples were analyzed as well (Tsunogai et al., 2010, 2011, 2014).

To determine whether the conversion rate from nitrate to N_2O was sufficient, the concentration of nitrate in the samples was determined each time we analyzed the

202 isotopic composition using CF-IRMS based on the N_2O^+ or O_2^+ outputs. We adopted
203 the $\delta^{15}N$, $\delta^{18}O$, and $\Delta^{17}O$ values only when the concentration measured via CF-IRMS
204 correlated with the concentration measured via ion chromatography prior to isotope
205 analysis within a difference of 10 %.

206 Three kinds of the local laboratory nitrate standards were used to determine the
207 isotopic compositions of stream nitrate, which had been named to be GG01 ($\delta^{15}N$ = –
208 3.07 ‰, $\delta^{18}O$ = +1.10 ‰, and $\Delta^{17}O$ = 0 ‰), HDLW02 ($\delta^{15}N$ = +16.11 ‰, $\delta^{18}O$ = +22.
209 20 ‰), and NF ($\delta^{18}O$ = +54.14 ‰, $\Delta^{17}O$ = +19.16 ‰). Both GG01 and HDLW02 were
210 used to determine $\delta^{15}N$ and $\delta^{18}O$ of stream nitrate, and both GG01 and NF were used
211 to determine $\Delta^{17}O$ of stream nitrate. The standard errors of the mean in the isotopic
212 compositions ($\delta^{15}N$, $\delta^{18}O$, and $\Delta^{17}O$) determined through repeated measurements on
213 GG01 (n = 3), were ±0.17 ‰ for $\delta^{15}N$, ±0.25 ‰ for $\delta^{18}O$, and ±0.10 ‰ for $\Delta^{17}O$, during
214 the measurements in this study. We repeated the analysis of $\delta^{15}N$, $\delta^{18}O$, and $\Delta^{17}O$ values
215 for each sample at least three times to attain high precision. All samples had a nitrate
216 concentration of greater than 10 μM, which corresponded to a nitrate quantity greater
217 than 100 nmol in a 10 mL sample. Thus, all isotope values presented in this study have
218 an error (standard error of the mean) better than ±0.2 ‰ for $\delta^{15}N$, ±0.3 ‰ for $\delta^{18}O$, and
219 ±0.1 ‰ for $\Delta^{17}O$.

220 Nitrite (NO_2^-) in the samples interferes with the final N_2O produced from nitrate
221 because the chemical method also converts NO_2^- to N_2O (McIlvin and Altabet, 2005).
222 Therefore, it is sometimes necessary to remove NO_2^- prior to converting nitrate to N_2O.

223 However, in this study, all the stream and soil water samples analyzed for stable isotopic
224 composition had NO_2^- concentrations lower than the detection limit (0.05 μM).
225 Because the minimum nitrate concentration in the samples was 24.7 μM in this study,
226 the ratios of NO_2^- to nitrate in the samples must be less than 0.2 %. Thus, we skipped
227 the processes for removing NO_2^-.
228
229 2.5 Calculating of the concentration of unprocessed $NO_3^-{}_{atm}$ in stream water
230 The $\Delta^{17}O$ data of nitrate in each sample can be used to estimate the concentration of
231 $NO_3^-{}_{atm}$ ($[NO_3^-{}_{atm}]$) in the stream water samples by applying Eq. (2):
232 $$[NO_3^-{}_{atm}]/[NO_3^-] = \Delta^{17}O/\Delta^{17}O_{atm} \quad (2)$$
233 where $[NO_3^-{}_{atm}]$ and $[NO_3^-]$ denote the concentration of $NO_3^-{}_{atm}$ and nitrate (total) in
234 each water sample, respectively, and $\Delta^{17}O_{atm}$ and $\Delta^{17}O$ denote the $\Delta^{17}O$ values of
235 $NO_3^-{}_{atm}$ and nitrate (total) in the stream water sample, respectively. In this study, we
236 used the average $\Delta^{17}O$ value of $NO_3^-{}_{atm}$ determined at the nearby Sado-Seki monitoring
237 station during the observation from April 2009 to March 2012 ($\Delta^{17}O_{atm}$ = +26.3 ‰;
238 Tsunogai et al., 2016) for $\Delta^{17}O_{atm}$ in Eq. (2) to estimate $[NO_3^-{}_{atm}]$ in the stream. We
239 allow for an error range in of 3 ‰ in $\Delta^{17}O_{atm}$, in which the factor changes in $\Delta^{17}O_{atm}$
240 from +26.3 ‰ caused by both areal and seasonal variation in the $\Delta^{17}O$ values of $NO_3^-{}_{atm}$
241 have been considered (Nakagawa et al., 2018; Tsunogai et al., 2016).
242
243

Table 1. Information on the samples taken during the intensive observation.

Storm event	Start time	End time	Date of filtration	Maximum period of storage without filtration
I	2019/8/22 16:00	2019/8/23 15:00	2019/8/29	7 days
II	2019/10/12 15:00	2019/10/13 14:00	2019/10/23	11 days
III	2020/9/13 11:00	2020/9/14 10:00	2020/9/25	12 days

3 Results

3.1 Variation during the routine observation

During the routine observation, the concentrations of stream nitrate ranged from 35.7 μM to 129.3 μM with the flux-weighted average concentration of 55.6 μM (Fig. 2a), showing little temporal changes from that determined during the past observations from 2013 to 2014 at the same catchment (58.4 μM; Nakagawa et al., 2018). The variation range also agreed with the past observation done in the same catchment (Kamisako et al., 2008), except for the extraordinarily large concentration (129.3 μM) recorded on 2018/8/31, which exceeded the 2σ of the whole variation range of stream nitrate of our routine observation (Fig. 2a). We will discuss the reason in section 4.2.

The stable isotopic compositions of stream nitrate during the routine observation ranged from +0.1 ‰ to +5.9‰ for $\delta^{15}N$ (Fig. 2b), from −1.9 ‰ to +7.7 ‰ for $\delta^{18}O$ (Fig. 2c), and from +0.4 ‰ to +2.7 ‰ for $\Delta^{17}O$ (Fig. 2d), while showing little seasonal variation. The flux-weighted averages for the $\delta^{15}N$, $\delta^{18}O$, and $\Delta^{17}O$ values of nitrate were +2.0 ‰, +1.1 ‰, and +1.1 ‰, respectively. Except for the extraordinarily large $\delta^{18}O$ and $\Delta^{17}O$ values we found on 2019/1/31 ($\delta^{18}O$ = +7.7 ‰ and $\Delta^{17}O$ = +2.7 ‰)

(Figs. 2c and 2d), the values are typical for stream nitrate eluted from temperate forested catchments (Hattori et al., 2019; Huang et al., 2020; Nakagawa et al., 2013, 2018; Riha et al., 2014; Sabo et al., 2016; Tsunogai et al., 2014, 2016). On the other hand, the data recorded on 2019/1/31 exceeded the 2σ variation range of the whole $\delta^{18}O$ and $\Delta^{17}O$ data. We will discuss the reason in section 4.3.

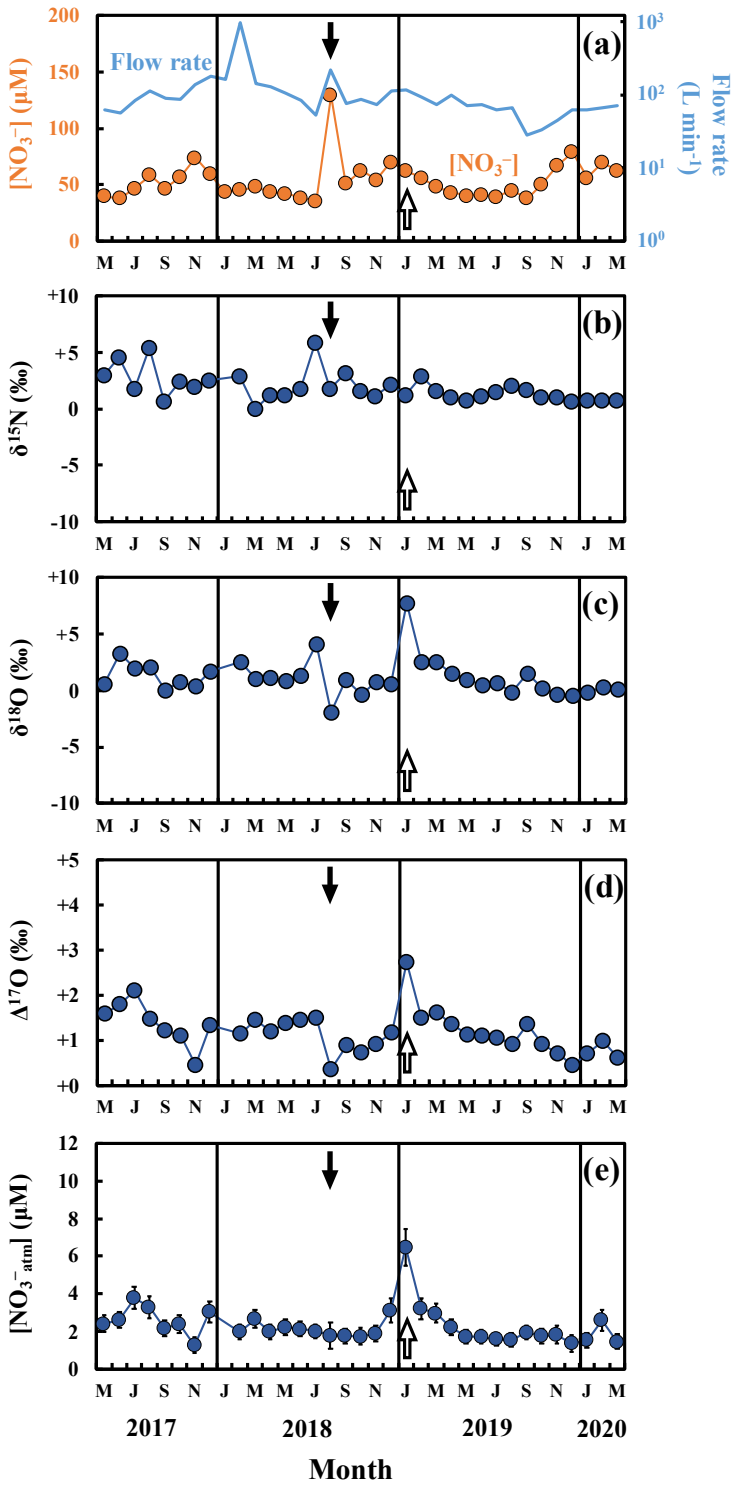

Figure 2. Temporal variations in the concentrations of nitrate (orange circles) and the flow rates (blue line) in the stream water during the routine observation (a), together with those of the values of $\delta^{15}N$ (b), $\delta^{18}O$ (c), $\Delta^{17}O$ (d) of nitrate, and the concentrations

of unprocessed atmospheric nitrate ([$NO_3^-{}_{atm}$]) (e) in the stream water (blue circles). The black and white arrows in the figures indicate the sampling that took place on 2018/8/31 and 2019/1/31, respectively. The error bars smaller than the sizes of the symbols are not presented.

3.2 Variation in response to the storm events

During the intensive observations made in response to the storm events, the concentration of stream nitrate showed significant short-term variation, from 24.7 μM to 122.6 μM, from 28.7 μM to 134.1 μM, and from 46.6 μM to 114.5 μM during the storm events I, II, and III, respectively, with the minimum recorded just before the beginning of each storm event and the maximum recorded when the flow rate was close to the maximum within each storm event (Figs. 3 and S1). Similar increase in the concentrations of stream nitrate in accordance with the increase in the flow rate during storm events have been reported in many past studies (e.g. Burns et al.,2019; Chen et al., 2020; Kamisako et al., 2008; Christopher et al., 2008). Especially, Kamisako et al. (2008), who monitored temporal changes in the concentration of stream nitrate in the same KJ catchment from 2003 to 2005 and found 11 nitrate increase events in accordance with the increase in the flow rate, reported the largest concentration of stream nitrate during the events to be 120 μM. The pattern and range of the short-term variation of the stream nitrate concentration during the three storm events were also consistent with the past study (Kamisako et al., 2008).

The stable isotopic compositions of stream nitrate during the three storm events also showed significant temporal variation, from −0.1 ‰ to +2.5 ‰, from −0.5 ‰ to +3.0 ‰, and from −0.1 ‰ to +3.5 ‰ for $\delta^{15}N$ (Figs. 3b, S1b, and S1g), from −3.4 ‰ to +3.1 ‰, from −2.5 ‰ to +2.9 ‰, and from −2.3 ‰ to +2.1 ‰ for $\delta^{18}O$ (Figs. 3c, S1c, and S1h), and from +0.3 ‰ to +1.6 ‰, from +0.3 ‰ to +1.4 ‰, and from +0.5 ‰ to +1.2 ‰ for $\Delta^{17}O$ (Figs. 3d, S1d, and S1i), with minimum values observed when the concentration of stream nitrate was at maximum and maximum values observed when the concentration of stream nitrate was at a minimum.

300

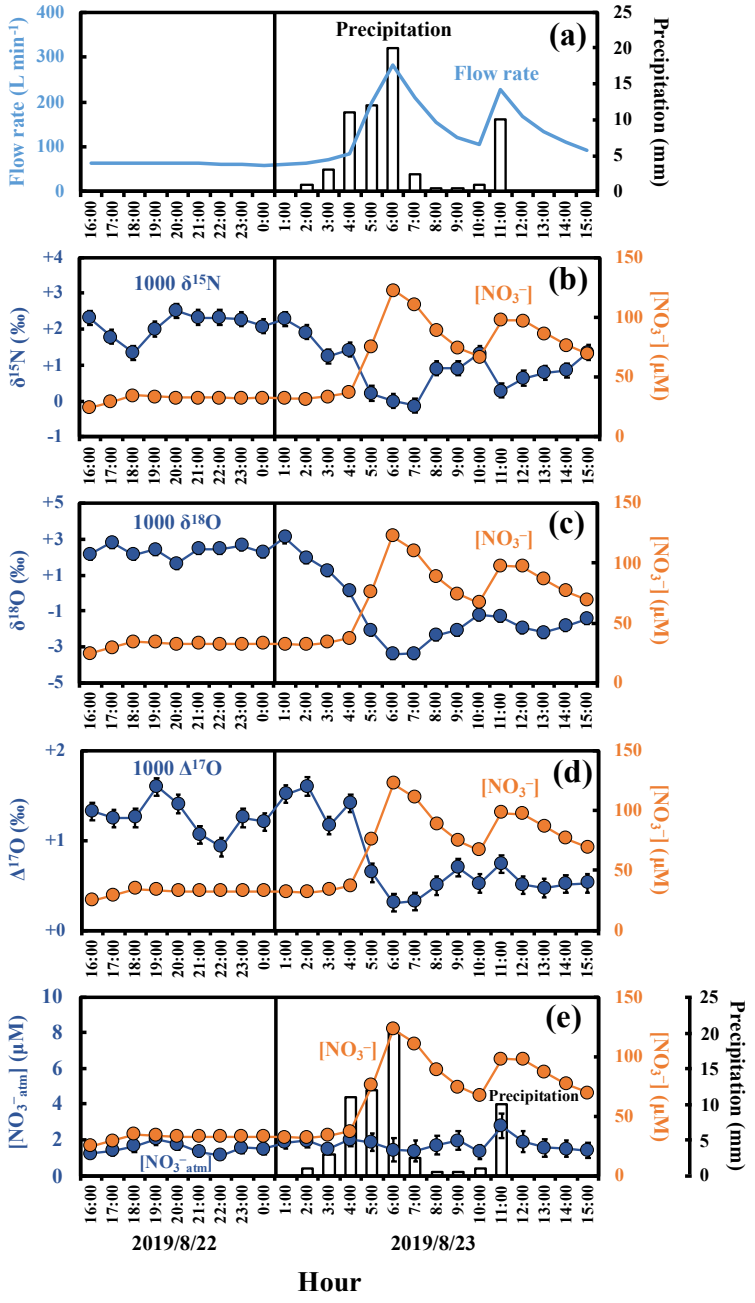

301 **Figure 3.** Temporal variations in the amount of precipitation (bar chart) and flow rates
302 of the stream water (blue line) during storm event I (a), together with those in the
303 concentrations of nitrate (orange circles) (b-e), the values of $\delta^{15}N$ (b), $\delta^{18}O$ (c), $\Delta^{17}O$ (d)
304 of nitrate, and $[NO_3^-{}_{atm}]$ (e) in the stream water (blue circles). The error bars smaller
305 than the sizes of the symbols are not presented.

306

307 **4 Discussion**

308 4.1 Possible alterations to the concentration and isotopic compositions of stream nitrate
309 during the storage period in the automatic sampler used for the intensive observations

310 During the intensive observations, the stream water samples were stored in bottles of
311 the automatic sampler. The storage periods until filtration were ranged from 7 (storm
312 event I) to 12 days (storm event III) (Table 1). While the automatic sampler was
313 surrounded by ferns and the other understory vegetations to minimize the possible
314 alterations on the samples, progress of biogeochemical reactions such as nitrification,
315 denitrification, and assimilation could alter the concentration and isotopic compositions
316 ($\delta^{15}N$, $\delta^{18}O$, and $\Delta^{17}O$) of stream nitrate during the storage period. Above all, possible
317 increase in soil water input into the stream water that is enriched with organic matters
318 during a storm event could enhance nitrification during the storage period and could
319 increase the concentration of nitrate in the stream water samples taken by using the
320 automatic sampler.

321 As a result, we discussed the possible alteration of the concentration and isotopic
322 compositions during the storage for the samples taken by using the automatic sampler
323 and concluded that the alterations during the storage in the automatic sampler were
324 minor in the samples. The details are described in Appendix A.

325 4.2 Primary source of nitrate increased during storm events

326 The striking feature of the observed short-term variation was that all the stable

isotopic compositions ($\delta^{15}N$, $\delta^{18}O$, and $\Delta^{17}O$) varied in response to the variation in the nitrate concentration throughout the three storm events (Figs. 3 and S1). The result implied that the source of increased nitrate during the storm events were different from that during the base flow period.

As a result, the stable isotopic compositions ($\delta^{15}N$, $\delta^{18}O$, and $\Delta^{17}O$) of stream nitrate were plotted as the functions of the reciprocal of the stream nitrate concentration ($1/[NO_3^-]$) for each storm event (Fig. 4). All the stable isotopic compositions of stream nitrate showed strong linear relationships ($R^2 > 0.5$; $p < 0.001$) with the reciprocal of concentrations. The linear relationships strongly suggest mixing between two endmembers with distinctively different isotopic signatures (e.g. Keeling, 1958). The observed strong linear relationships not only in the $\Delta^{17}O$ of stream nitrate (Figs. 4g, 4h, and 4i), which is stable during the progress of partial removal reactions such as denitrification or assimilation, but also in the $\delta^{15}N$ and $\delta^{18}O$ of stream nitrate (Figs. 4a-4f), which should be altered during the progress of the partial removal reactions, also implied that the progress of denitrification or assimilation in bottles of the automatic sampler during the storage period without filtration were minor in the samples.

The nitrate-depleted endmember must be the source of stream nitrate during the base flow period prior to each storm event. On the other hand, the nitrate-enriched endmember represents the source of nitrate that was added during the storm events.

Atmospheric nitrate ($NO_3^-{}_{atm}$) dissolved in rainwater was one of the possible sources of nitrate enriched during the storm events (Inamdar and Mitchell, 2006). While the $NO_3^-{}_{atm}$ showed the $\delta^{18}O$ and $\Delta^{17}O$ values enriched in both ^{18}O and ^{17}O, more than +55 ‰ and more than +18 ‰, respectively, during summer periods in Japan (Tsunogai et al., 2016), the nitrate-enriched endmember showed the $\delta^{18}O$ and $\Delta^{17}O$ values depleted in both ^{18}O and ^{17}O, less than +3.1 ‰ and +1.6 ‰, respectively, during the storm events. During storm events, increase in $\delta^{18}O$ and/or $\Delta^{17}O$ have been reported for stream nitrate eluted from forested catchments in past studies (Sebestyen et al., 2019; Sabo et al., 2016; Buda and Dewalle. 2009). In KJ catchment, however, we found significant decrease in both the $\delta^{18}O$ and $\Delta^{17}O$ of stream nitrate during storm events. In addition, the concentrations of $NO_3^-{}_{atm}$ ($[NO_3^-{}_{atm}]$) showed little temporal variations showing the concentrations of 1.6 ± 0.4 μM, 1.8 ± 0.4 μM, and 2.1 ± 0.4 μM during the storm events I, II, and III, respectively (Figs. 3e, S1e, and S1j). In general, the $[NO_3^-{}_{atm}]$ in rainwater were much higher than those in stream water (Nakagawa et al., 2018; Rose et al., 2015; Tsunogai et al., 2014). During the storm events I, II, and III, however, the $[NO_3^-{}_{atm}]$ in stream water was almost constant irrespective to the increase in precipitation (Figs. 3e, S1e, and S1j). Thus, we conclude that the direct input of $[NO_3^-{}_{atm}]$ via rainwater into the stream through overland flow during storm events can be negligible, at least in the KJ catchment. Thus, we concluded that the $NO_3^-{}_{atm}$ should be the minor source of nitrate that increased during the storm events.

Nakagawa et al. (2018) determined the temporal variations in the concentrations (Fig. 5a) and isotopic compositions ($\delta^{15}N$, $\delta^{18}O$, and $\Delta^{17}O$) (Figs. 5b, 5c, and 5d) of soil nitrate dissolved in soil water taken within the same catchment during 2013 to 2014, at the depths of 20 cm and 60 cm of the station SLS (SLS 20 and SLS 60, respectively) and at the depth of 20 cm of the station SMS (SMS 20), where the station SLS was located in the riparian zone of the stream and the station SMS was about 20 m away from the stream and located in the upland zone (Fig. 1b). The concentrations of soil nitrate showed significant seasonal variation, with the higher concentration in summer and the lower concentration in winter (Fig. 5a). Both the $\delta^{18}O$ and $\Delta^{17}O$ values also showed significant seasonal variation, with the minimum in summer and the maximum in winter (Figs. 5c and d). To verify if the soil nitrate is the source of the stream nitrate that was added to the stream during the storm events, we also plotted soil nitrate at each site (SLS 20, SLS 60 and SMS 20) of the same season in Fig. 4. Because our intensive observations on the storm events were done in summer (from August to October), the average concentration and the average isotopic composition during summer (from August to October) were calculated (Table 2) and plotted in Fig. 4. The error bars of each soil nitrate denote the standard deviation (SD) of each isotopic composition (n =5 for each). We found that the isotopic compositions ($\delta^{15}N$, $\delta^{18}O$, and $\Delta^{17}O$) of soil nitrate in the riparian zone (SLS 20 and SLS 60; Table 2) were always plotted on the nitrate-enriched extension (lower $1/[NO_3^-]$ extension) of the mixing line during the storm events I, II, and III (Fig. 4), while those of the soil

389 nitrate in the upland zone (SMS 20; Table 2) were somewhat deviated from the
390 nitrate-enriched extension of the mixing line, $\delta^{18}O$ especially (Figs. 4d, 4e, and 4f).
391 We conclude that the primary source of nitrate added during the storm events was the
392 soil nitrate in the riparian zone.

393 The "flushing hypothesis" has been proposed to explain the increase in stream
394 nitrate concentration in accordance with the increase in flow rate during storm events
395 (Creed et al., 1996; Hornberger et al., 1994). During the base flow periods, nitrate
396 accumulate in shallow, oxic soil layers due to the progress of nitrification. When
397 water level became higher during storm periods, concentration of stream nitrate
398 increased due to flushing of the soil nitrate accumulated in the shallow soil layers of
399 riparian zones into stream (Chen et al., 2020; Creed et al., 1996; Ocampo et al., 2006).
400 Our finding that the primary source of nitrate increased during the storm events was
401 the soil nitrate in the riparian zone is consistent with the "flushing hypothesis." We
402 conclude that the flushing of soil nitrate in the riparian zone into the stream due to
403 rising of both stream water and groundwater level was primarily responsible for the
404 increase in stream nitrate during the storm events (Fig. 6).

405 Within the whole dataset on the variation of the concentration of nitrate in the stream
406 determined by Kamisako et al. (2008), increases in the concentration of stream nitrate
407 to more than 20 μM in response to storm events were limited to the storm events that
408 occurred in the warm months, from June to November. As the concentrations of soil
409 nitrate in the riparian zone (SLS 20 and SLS 60) were much higher in the warm months

410 (734 μM ± 496 μM; from June to November) than in the cold months (156 ± 124 μM;
411 from December to May), such seasonal variation in the concentration of riparian soil
412 nitrate is consistent with the observed seasonality in the influence of storm events on
413 the stream nitrate concentration, where significant increase were limited to warm
414 months, whereas insignificant effects are observed during cold months.

415 The stream nitrate during storm events showed $\delta^{15}N$ values more depleted in ^{15}N than
416 those during the base flow periods (Figs. 3b, S1b, and S1g), probably due to the input
417 of riparian soil nitrate more depleted in ^{15}N. Compared with the $\delta^{15}N$ values of stream
418 nitrate taken during the base flow periods of routine observations when precipitation
419 was less than 1 mm/day (Fig. 2b; Table S1), the riparian soil nitrate (SLS 20 and SLS
420 60; Table 2) showed the $\delta^{15}N$ values around 3.5 ‰ lower. The trend and the extent of
421 the ^{15}N-depletion coincided well with those determined in the forested catchments in
422 past studies (Fang et al., 2015; Hattori et al., 2019). Fang et al. (2015), for instance,
423 reported significant differences between the $\delta^{15}N$ values of soil nitrate and those of
424 stream nitrate in six forested catchments in Japan and China, and proposed that the
425 kinetic fractionation due to the progress of denitrification during the elution of soil
426 nitrate into groundwater was responsible for the relative ^{15}N-enrichment in stream
427 nitrate compared with soil nitrate. As a result, the observed temporal decrease in the
428 $\delta^{15}N$ value of stream nitrate during storm events also supported that the flushing of soil
429 nitrate showing ^{15}N-depleted $\delta^{15}N$ values into the stream was responsible for the
430 elevated of nitrate concentrations during storm events.

As mentioned in section 3.1, we found significant increase in nitrate concentration up to 129.3 μM on 2018/8/31 during our routine observation on the stream, when the water was sampled in the middle of a heavy storm (48.0 mm/day; Table S1) with significant increase in flow rate (from 53.4 L/min one month before to 216.9 L/min during sampling), which the amount of precipitation on 2018/8/31 was the highest within the whole routine observations (Table S1). The measured $\delta^{18}O$ and $\Delta^{17}O$ value of the stream nitrate on 2018/8/31 (−1.9 ‰ and +0.4 ‰, respectively), showing significantly smaller values than those during the other routine observation (Fig. 2c and 2d), agreed well with those of the nitrate increase during the storm events I, II, and III. Moreover, both the range of increase in stream nitrate concentration (129.3 μM) and the season of observation (August) also agreed well with those of the stream nitrate increase during the three storm events. As a result, we conclude that the input of soil nitrate accumulated in the riparian zone due to flushing was also responsible for the significant increase in stream nitrate concentration we found on 2018/8/31 during the routine observation.

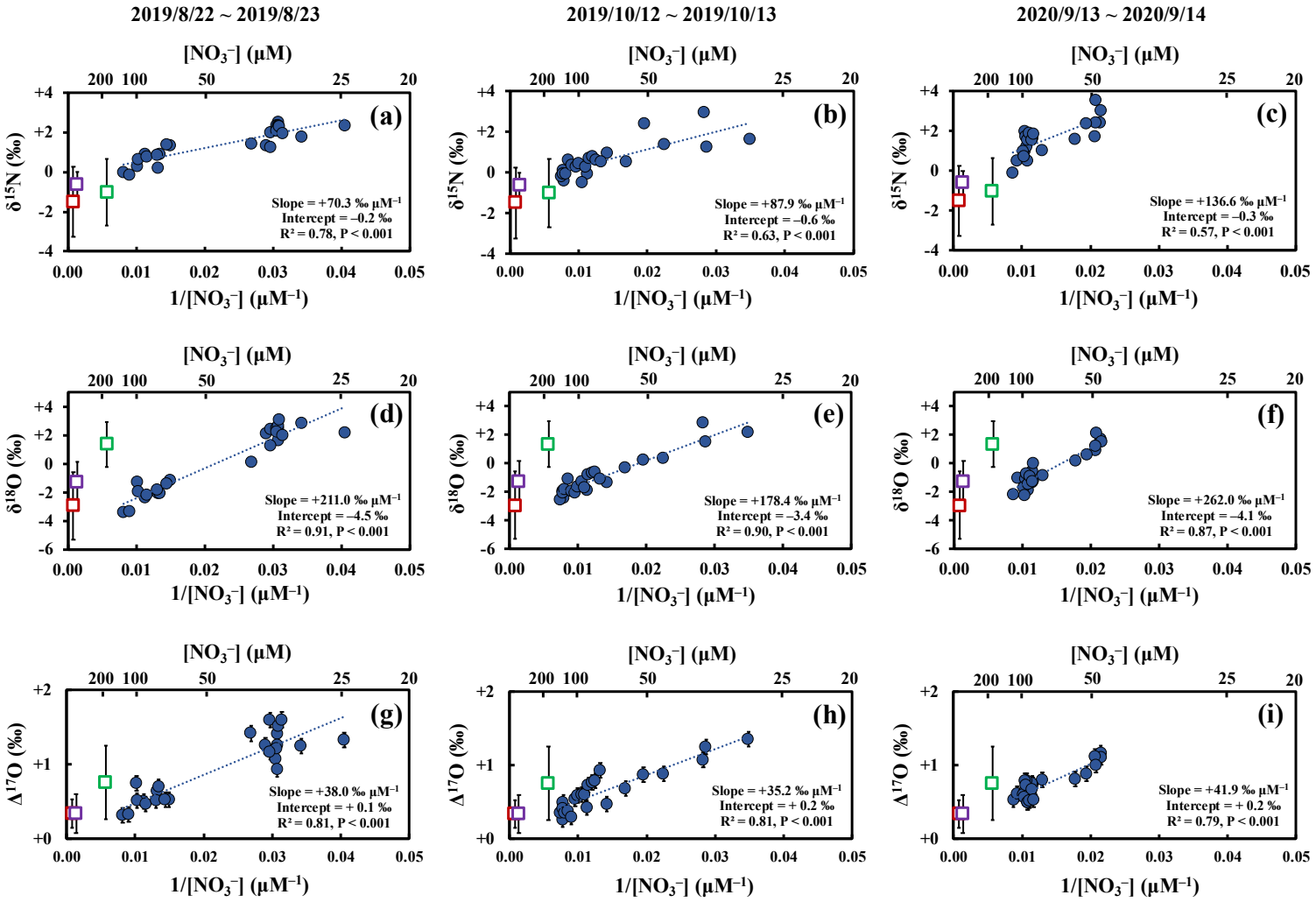

Figure 4. The $\delta^{15}N$ (a, b, and c), $\delta^{18}O$ (d, e, and f), and $\Delta^{17}O$ (g, h, and i) values of stream nitrate (blue circles) during storm events I, II, and III plotted as a function of the reciprocal of nitrate concentration ($1/[NO_3^-]$), together with those of soil nitrate at SLS 20 (red squares; riparian zone), SLS 60 (purple squares; riparian zone), and SMS 20 (green squares; upland zone) during August to October in 2013 and 2014. The error bars of each soil nitrate denote the standard deviation (SD) of each isotopic composition (n =5 for each). The error bars smaller than the sizes of the symbols are not presented.

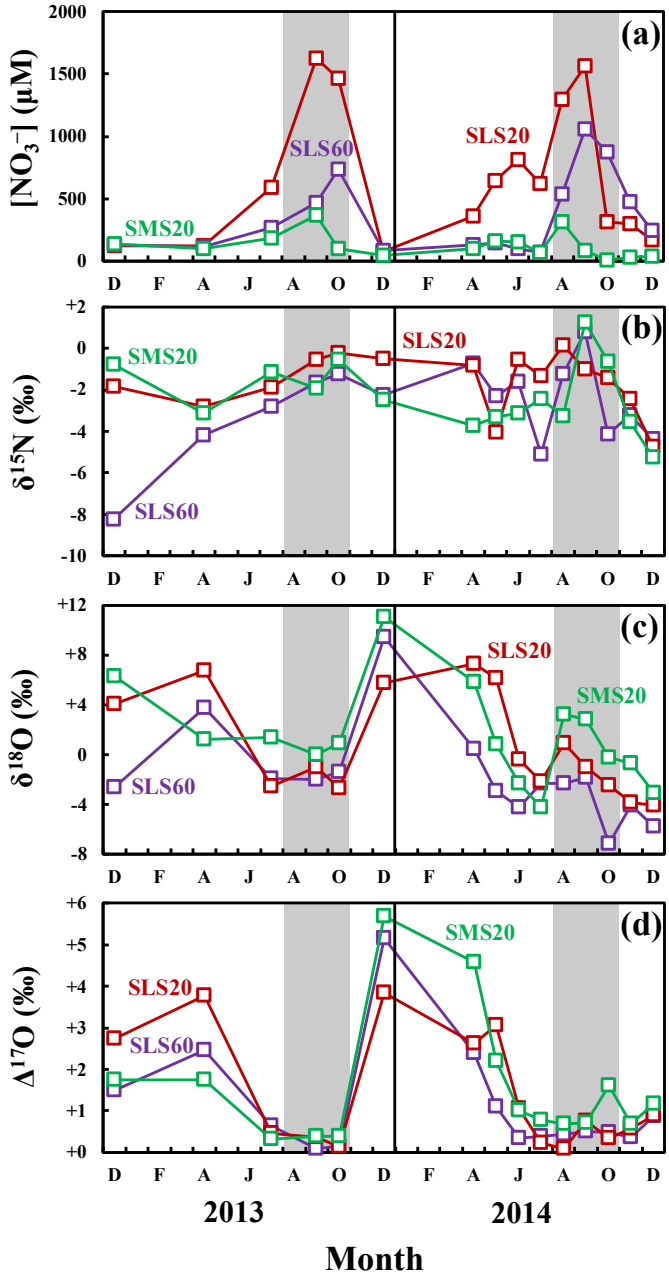

454 **Figure 5.** Seasonal variations in the concentrations of soil nitrate (a) at SLS 20 (red
455 squares), SLS 60 (purple squares), and SMS20 (green squares), together with those in
456 the values of $\delta^{15}N$ (b), $\delta^{18}O$ (c) and $\Delta^{17}O$ (d) of each soil nitrate during 2013 to 2014
457 (modified from Nakagawa et al., 2018). The periods used to estimate the isotopic
458 compositions (from August to October) are presented in gray. The error bars were
459 smaller than the sizes of the symbols.

460 **Table 2.** Concentrations and isotopic compositions ($\delta^{15}N$, $\delta^{18}O$, and $\Delta^{17}O$) of soil nitrate

461 at SLS 20, SLS 60, and SMS 20 during August to October in 2013 and 2014

462 (recalculated from the data in Nakagawa et al., 2018).

463

	SLS 20	SLS 60	SMS 20
NO_3^- (μM)	1254 ± 537	734 ± 241	176 ± 159
1000 $\delta^{15}N$	−1.5 ± 1.8	−0.6 ± 0.6	−1.0 ± 1.7
1000 $\delta^{18}O$	−2.9 ± 2.4	−1.3 ± 1.4	+1.4 ± 1.6
1000 $\Delta^{17}O$	+0.3 ± 0.2	+0.3 ± 0.3	+0.8 ± 0.5

464

465

466

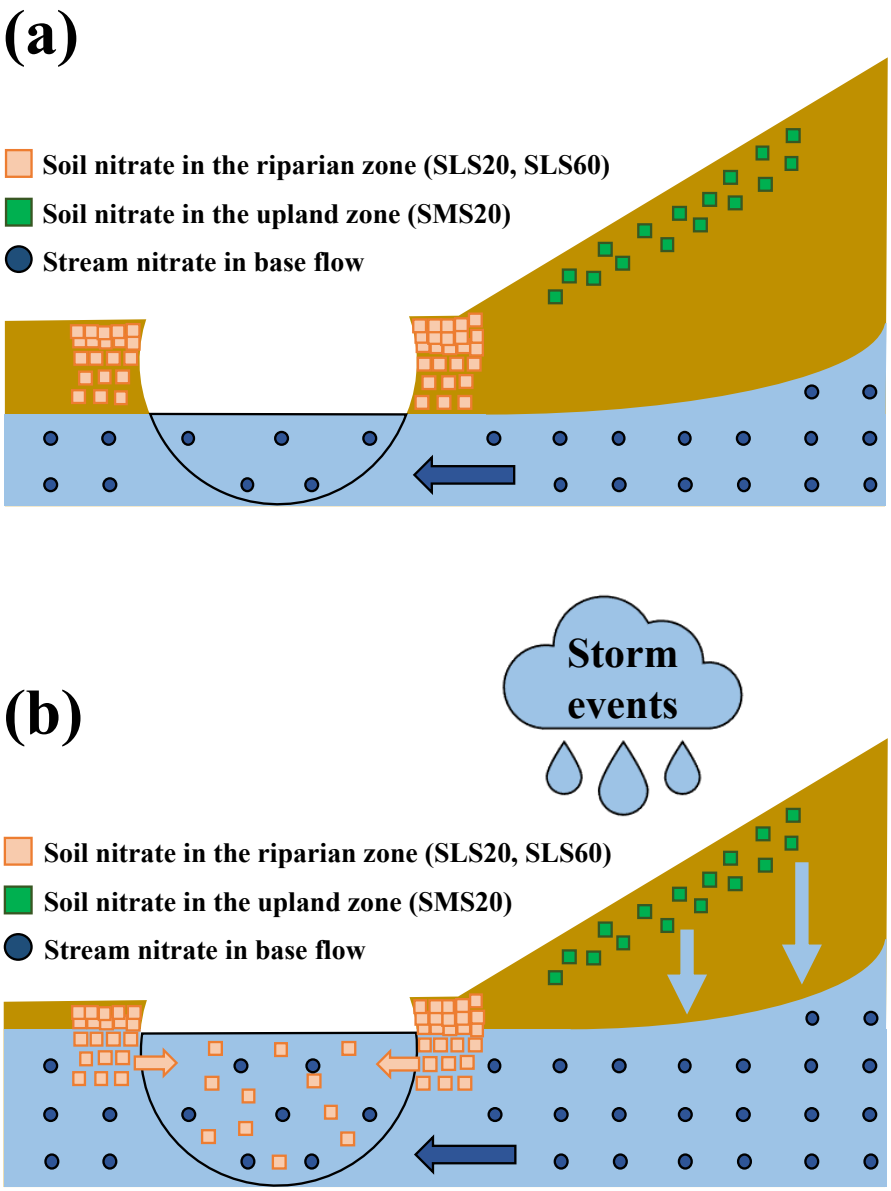

Figure 6. Schematic diagram showing the elution of soil nitrate to the stream before the storm events (a) and during the storm events (b). Soil nitrate in the riparian zone and that in the upland zone are represented by the orange squares and green squares, respectively, while stream nitrate during base flow is represented by the blue circles.

4.3 Variation in the concentration of $NO_3^-{}_{atm}$ during routine observation

The concentration of $NO_3^-{}_{atm}$ ($[NO_3^-{}_{atm}]$) showed little seasonal variation, from 1.3 μM to 3.8 μM during our routine observation in this study (Fig. 2e), except for the extraordinarily large $[NO_3^-{}_{atm}]$ we found on 2019/1/31 (6.5 μM). Except for the extraordinarily large $[NO_3^-{}_{atm}]$, the obtained $[NO_3^-{}_{atm}]$ corresponded well with those determined in the past study done at the same catchment (Nakagawa et al., 2018). In addition, they corresponded well with those of the temperate forested catchments saturated in nitrogen, such as Fernow experimental Forest 3 (4.2 μM; Rose et al., 2015).

In this study, accumulation of snow up to 18 cm was observed at the KJ catchment on 2019/1/27, while most of the accumulated snow had melted to a depth of 1 cm by 2019/1/30, just before the sampling on 2019/1/31. Furthermore, during the routine observation period from 2017/5 to 2020/3, no other snow-melting events occurred within 4 days prior to the day of sampling, except for the sampling on 2019/1/31. Similar enhancement in the concentration of $NO_3^-{}_{atm}$, as well as the $\delta^{18}O$ and $\Delta^{17}O$ of stream nitrate, in response to snow melting has been frequently observed in streams worldwide (Ohte et al., 2004, 2010; Pellerin et al., 2012; Piatek et al., 2005; Rose et al.,

2015; Sabo et al., 2016; Tsunogai et al., 2014, 2016).

The flow rate, concentration of stream nitrate, and $\Delta^{17}O$ was 110.0 L/min, 70.0 μM, and +1.17 ‰ on 2018/12/28, respectively, while 117.3 L/min, 62.4 μM, and +2.73 ‰ on 2019/1/31, respectively (Table S1). The $[NO_3^-{}_{atm}]$ in stream water was estimated to be 3.1 μM on 2018/12/28 and 6.5 μM on 2019/1/31. Assuming that the $[NO_3^-{}_{atm}]$ in snow melt was the same with the volume-weighted mean concentration of nitrate in rainwater (41.0 μM) determined at Sado island in January (EANET, 2010, 2011; Tsunogai et al., 2016), the increase in the flow rate ($\Delta F_{snowmelt}$) due to the mixing of snow melt into the stream can be estimated to be 10.3 L/min, by using the mass balance equation shown below:

$$[NO_3^-{}_{atm}]_{2019/1/31} \times F_{2019/1/31} = [NO_3^-{}_{atm}]_{2018/12/28} \times F_{2018/12/28} + [NO_3^-{}_{atm}]_{snowmelt} \times \Delta F_{snowmelt} \quad (3)$$

where $[NO_3^-{}_{atm}]_{2018/12/28}$, $[NO_3^-{}_{atm}]_{2019/1/31}$, and $[NO_3^-{}_{atm}]_{snowmelt}$ denote the $[NO_3^-{}_{atm}]$ in stream water on 2018/12/28, 2019/1/31, and that in snow melt water, respectively, and $F_{2018/12/28}$, $F_{2019/1/31}$, and $\Delta F_{snowmelt}$ denote the flow rate of stream water on 2018/12/28, 2019/1/31, and the increase in the flow rate due to snow melt, respectively. Because the estimated volume of melting snow water into the stream water (10.3 L/min) was comparable with the observed increase in the flow rate from 2018/12/28 to 2019/1/31 (7.3 L/min), we concluded that the snow melting was responsible for the increase in $\Delta^{17}O$ on 2019/1/31 and that the input of $NO_3^-{}_{atm}$ accumulated in the melted snow water, showing $\delta^{18}O$ and $\Delta^{17}O$ values significantly higher than those in the stream, caused the

509 extraordinarily increase in [$NO_3^-{}_{atm}$] on 2019/1/31. Except for the extraordinarily
510 increase in [$NO_3^-{}_{atm}$] (n = 1), [$NO_3^-{}_{atm}$] was stable at 2.2 ± 0.6 μM throughout the
511 routine observation (n = 33). We concluded that [$NO_3^-{}_{atm}$] was generally stable in the
512 stream.
513
514 4.4 The impact of storm events on the index of the nitrogen saturation
515 The concentration of stream nitrate eluted from a forested catchment has been used
516 as an index to evaluate the stage of nitrogen saturation (Huang et al., 2020; Rose et al.,
517 2015; Stoddard, 1994). However, McHale et al. (2002) pointed out the problem in the
518 reliability of this index, because the number of storm events influenced the
519 concentration of nitrate eluted from forested stream significantly. That is, if we use the
520 concentration of stream nitrate sampled during the storm events to evaluate the stage of
521 nitrogen saturation in a forested catchment, the stage of nitrogen saturation might be
522 overestimated.
523 Nakagawa et al. (2018) have proposed the export flux of $NO_3^-{}_{atm}$ (M_{atm}) relative to
524 the deposition flux of $NO_3^-{}_{atm}$ (D_{atm}) can be an alternative, more robust index for
525 nitrogen saturation in temperate forested catchments, because the M_{atm}/D_{atm} ratio
526 directly reflect the demand on atmospheric nitrate deposited onto each forested
527 catchments as a whole, and thus reflect the nitrogen saturation in each forested
528 catchment. To estimate reliable M_{atm} in each forested catchment, we must obtain
529 reliable [$NO_3^-{}_{atm}$] in the forested stream, including their temporal variation.

As already presented in section 4.2, we found that [$NO_3^-{}_{atm}$] remained almost constant irrespective to the significant variation in [NO_3^-] during storm events (Figs. 3e, S1e, and S1j). The concentrations of atmospheric nitrate ([$NO_3^-{}_{atm}$]) in rainwater were much higher than those in stream water. While the volume-weighted mean [$NO_3^-{}_{atm}$] in rainwater determined in Sado island from August to October, for example, was 15.2 ± 8.4 μM (EANET, 2010, 2011; Tsunogai et al., 2016), that in the stream water was 2.2 ± 0.6 μM in this study. As a result, the [$NO_3^-{}_{atm}$] in stream water would increase, if significant portion of rainwater was added directly into the stream water during the storm events. The [$NO_3^-{}_{atm}$] in stream water, however, was stable showing no correlation with the amount of precipitation or the concentration of stream nitrate during the storm events (Figs. 3e, S1e, and S1J). The [$NO_3^-{}_{atm}$] remained almost constant as well during the stream event on 2018/8/31 we found through the routine observation, while [NO_3^-] increased from 35.7 μM (1 month before) to 129.3 μM (Fig. 2e). As a result, we concluded that the direct input of $NO_3^-{}_{atm}$ into the stream water was negligible even during the storm events.

The observed [$NO_3^-{}_{atm}$] showing almost constant values implies that the primary source of $NO_3^-{}_{atm}$ in stream water during storm events was the $NO_3^-{}_{atm}$ stored in groundwater, which is the same source as that during the base flow periods, rather than the direct input of $NO_3^-{}_{atm}$ from rainwater. Because direct input of $NO_3^-{}_{atm}$ into stream water was negligible during the storm events, the M_{atm}/D_{atm} ratio in each forested catchment should be controlled by the metabolized processes (uptake or denitrification)

551 in each forested catchment subsequent to deposition, so that the M_{atm}/D_{atm} can correctly
552 reflect the total demand on $NO_3^-{}_{atm}$ in each forested catchment and thus the status of
553 nitrogen saturation. We conclude that the M_{atm}/D_{atm} ration can be a more robust index
554 to evaluate nitrogen saturation in forested catchments.
555
556 **5 Conclusions**
557 Temporal variations in the concentrations and stable isotopic compositions ($\delta^{15}N$,
558 $\delta^{18}O$, and $\Delta^{17}O$) of stream nitrate were determined during storm events to clarify the
559 source of stream nitrate increased during storm events. Because the stable isotopic
560 compositions of soil nitrate in riparian zone during summer agreed well with those of
561 the nitrate-enrich endmember of the stream nitrate increased during storm events, we
562 conclude that the soil nitrate in riparian zone was primarily responsible for the stream
563 nitrate increase during storm events. Additionally, the concentration of $NO_3^-{}_{atm}$ in the
564 stream was almost constant during the storm events, implied that the source of $NO_3^-{}_{atm}$
565 in stream water during storm events was the $NO_3^-{}_{atm}$ stored in groundwater. We
566 concluded that the number of storm events have little impact on M_{atm}/D_{atm} ratio, the
567 index of nitrogen saturation. In addition, the $\Delta^{17}O$ of nitrate can be applicable as the
568 tracer to clarify the source of nitrate.
569
570
571

Appendix A: Possible alterations to the concentration and isotopic compositions of stream nitrate during the storage period in the automatic sampler used for the intensive observations

During the intensive observations, the stream water samples were stored in bottles of the automatic sampler. The storage periods until filtration were ranged from 7 (storm event I) to 12 days (storm event III) (Table 1). While the automatic sampler was surrounded by ferns and the other understory vegetations to minimize the possible alterations on the samples, progress of biogeochemical reactions such as nitrification, denitrification, and assimilation could alter the concentration and isotopic compositions ($\delta^{15}N$, $\delta^{18}O$, and $\Delta^{17}O$) of stream nitrate during the storage period. Above all, possible increase in soil water input into the stream water that is enriched with organic matters during a storm event could enhance nitrification during the storage period and could increase the concentration of nitrate in the stream water samples taken by using the automatic sampler. Here, we discussed the possible alteration of the concentration and isotopic compositions during the storage for the samples taken by using the automatic sampler.

First, we compared the samples taken during the intensive observations using the automatic sampler with those taken during the routine observations. During the routine observations, the stream water samples were taken manually, transported to the laboratory within 1 h of each collection, passed through a membrane filter (pore size 0.45 μm), and stored in a refrigerator (4°C) until chemical analysis. As a result,

593 alterations should be minor in the samples taken through the routine observations.

594 When we compared the concentrations and isotopic compositions of stream nitrate
595 in the samples taken at the beginning of the intensive observation using the automatic
596 sampler with those in the routine observation nearby, they coincided well each other
597 (Table A1), implying that at least the progress of nitrification within the bottles of the
598 automatic sampler should be minor during the storage period because the concentration
599 of nitrate should increase, while the $\Delta^{17}O$ should decreased significantly during the
600 storage period if the progress of nitrification was active in the bottles of the intensive
601 observation.

602 In addition, a clear storm event was also observed during the routine observation on
603 2018/8/31 (Fig. 2; Table S1), so that we can compare the concentrations and isotopic
604 compositions of stream nitrate with those of intensive observations. During the routine
605 observation on 2018/8/31 done under a precipitation and flow rate of 48 mm/day and
606 216.9 L/min, respectively, we observed a significant increase in the concentration of
607 stream nitrate from 35.7 μM one month before to 129.3 μM (Fig. 2 and Table S1). In
608 accordance with the increase in the concentration, we found significant changes in the
609 isotopic compositions; from +5.9 ‰ to +1.8 ‰ for $\delta^{15}N$, from +4.1 ‰ to –1.9 ‰ for
610 $\delta^{18}O$, from +1.5 ‰ to +0.4 ‰ for $\Delta^{17}O$ (Fig. 2 and Table S1). The trend and the degree
611 of the variations in the concentration and the isotopic compositions on 2018/8/31 from
612 those on one month before were consistent with those of the intensive observation (Figs.
613 3 and S1). As a result, we concluded that the increase in the flow rate was responsible

for the observed increase in concentrations of stream nitrate during the storm events and thus the microbial production of nitrate through nitrification during the storage had little influence on the observed temporal changes in the concentrations and isotopic compositions of nitrate in the stream water samples taken by using the automatic sampler.

Kotlash and Chessman (1998) conducted storage experiments under various conditions such as freezing, acidification, refrigeration, and room temperature to clarify the changes in the concentrations of nitrogen compounds in stream water samples and found little change in concentration of oxidized nitrogen (NO_3^- + NO_2^-) irrespective of the treatments. To further verify the insignificant changes in the concentrations and isotopic compositions of stream nitrate stored without treatments in the samples taken by the automatic sampler, we also conducted the storage experiments by using a 100 mL of stream water taken at the KJ forested catchment on 2022/4/28 and stored in a 100 ml PP (polypropylene) bottle without treatments. Approximately 85 mL of the stream water within the bottle was filtered using a GF/F filter paper (25 mm diameter) and stored in a refrigerator (4°C) to determine original (initial) concentration and isotopic compositions of nitrate. To simulate the stream water containing increased suspended organic matters during the storm events, the GF/F filter paper was returned to the 100 mL PP bottle which contained 15 mL of the stream water sample and left the 15 mL stream water under the room temperature (18.3°C) for 2 weeks together with the suspended organic matters on the filter. The concentration and isotopic compositions of

635 the original stream nitrate (85 mL) and those being stored without filtration under the
636 room temperature for 2 weeks (15 mL) were analyzed by using the same method
637 presented in section 2.4. The concentration of nitrate in the stream water sample being
638 stored for 2 weeks without treatments coincided well with those in the original, showing
639 the difference in concentrations less than 10 % (Table A2). Besides, the differences in
640 the isotopic compositions from the original were also negligibly small (Table A2).
641 As a result, we concluded that the possible alteration in the concentration and isotopic
642 compositions of nitrate due to the progress of biogeochemical reactions such as
643 nitrification, denitrification, and assimilation during storage in the automatic sampler
644 used in the intensive observations was negligibly small.
645
646
647
648
649
650
651
652
653
654
655

Table A1. Comparison of both concentration and isotopic compositions ($\delta^{15}N$, $\delta^{18}O$, and $\Delta^{17}O$) of stream nitrate between those taken at the beginning of intensive observations using the automatic sampler and those taken manually on the days nearby during routine observations.

	Type	Flow rate L/min	Precipitation mm/day	NO_3^- μM	$\delta^{15}N$ /10^3	$\delta^{18}O$ /10^3	$\Delta^{17}O$ /10^3
2019/7/31	routine	61.6	0.0	39.5	+1.55	+0.66	+1.06
2019/8/22 16:00	intensive	64.1	1.0	24.7	+2.32	+2.17	+1.33
2019/8/30	routine	66.0	13.0	44.9	+2.07	−0.13	+0.91
2019/9/30	routine	28.0	0.0	37.9	+1.65	+1.56	+1.36
2019/10/12 15:00	intensive	22.4	7.0	28.7	+1.61	+2.18	+1.35
2019/10/31	routine	32.6	0.0	50.4	+1.04	+0.19	+0.92
2020/9/13 11:00	intensive	111.0	0.0	46.6	+2.42	+1.74	+1.17
2020/9/30	routine	117.3	0.0	63.2	–	–	–

−:No samples were taken for isotopic analysis

Table A2. Comparison of both concentration and isotopic compositions ($\delta^{15}N$, $\delta^{18}O$, and $\Delta^{17}O$) between original stream water sample and that being stored under the room temperature for 2 weeks without treatments.

	NO_3^- μM	$\delta^{15}N$ /10^3	$\delta^{18}O$ /10^3	$\Delta^{17}O$ /10^3
Original	53.2	+0.90	+0.80	+1.05
Stored	49.5	+0.85	+0.90	+0.99

Data availability. All the primary data are presented in the Supplement. The other data are available upon request to the corresponding author (Weitian Ding).

Author contributions. WD, UT, NY, and HS designed the study. HY, MM, and HS performed the field observations. HY, MM, and HS determined the concentrations of the samples. WD determined the isotopic compositions of the samples. WD, TS, FN, and UT performed data analysis, and WD and UT wrote the paper with input from MM, HY and HS.

Competing interests. The authors declare that they have no conflict of interest.

Acknowledgements.

We thank anonymous referees for valuable remarks on an earlier version of this paper. The samples analyzed in this study were collected through the Long-term Monitoring of Transboundary Air Pollution and Acid Deposition by the Ministry of the Environment in Japan. The authors are grateful to Ryo Shingubara, Masanori Ito, Hao Xu, Hui Lan, Peng Lai, Tianzheng Huang, Yuhei Morishita, Tae Ito, Yuka Tadachi and other present and past members of the Biogeochemistry Group, Nagoya University, for their valuable support throughout this study. This work was supported by a Grant-in-Aid for Scientific Research from the Ministry of Education, Culture, Sports, Science, Technology of Japan under grant numbers JP17H00780, JP19H04254, and JP19H00955, the Yanmar Environmental Sustainability Support Association, and the River Fund of The River Foundation, Japan. Weitian Ding would

like to take this opportunity to thank the 'Nagoya University Interdisciplinary Frontier Fellowship' supported by JST and Nagoya University.

Reference

Aber, J. D., Nadelhoffer, K. J., Steudler, P. and Melillo, J. M.: Nitrogen Saturation in Northern Forest Ecosystems, Bioscience, 39(6), 378–386, doi:10.2307/1311067, 1989.

Aguilera, R. and Melack, J. M.: Concentration-Discharge Responses to Storm Events in Coastal California Watersheds, Water Resour. Res., 54(1), 407–424, doi:10.1002/2017WR021578, 2018.

Alexander, B., Hastings, M. G., Allman, D. J., Dachs, J., Thornton, J. A. and Kunasek, S. A.: Quantifying atmospheric nitrate formation pathways based on a global model of the oxygen isotopic composition ($\delta^{17}O$) of atmospheric nitrate, Atmos. Chem. Phys., 9(14), 5043–5056, doi:10.5194/acp-9-5043-2009, 2009.

Buda, A. R. and DeWalle, D. R.: Dynamics of stream nitrate sources and flow pathways during stormflows on urban, forest and agricultural watersheds in central Pennsylvania, USA, Hydrol. Process., 23(23), 3292–3305, doi:https://doi.org/10.1002/hyp.7423, 2009.

Burns, D. A. and Kendall, C.: Analysis of $\delta^{15}N$ and $\delta^{18}O$ to differentiate NO_3^- sources in runoff at two watersheds in the Catskill Mountains of New York, Water Resour. Res., 38(5), 91–912, doi:10.1029/2001wr000292, 2002.

Burns, D. A., Pellerin, B. A., Miller, M. P., Capel, P. D., Tesoriero, A. J. and Duncan, J. M.: Monitoring the riverine pulse: Applying high-frequency nitrate data to advance integrative understanding of biogeochemical and hydrological processes, Wiley Interdiscip. Rev. Water, (October 2018), e1348, doi:10.1002/wat2.1348, 2019.

Chen, X., Tague, C. L., Melack, J. M. and Keller, A. A.: Sensitivity of nitrate concentration-discharge patterns to soil nitrate distribution and drainage properties in the vertical dimension, Hydrol. Process., 34(11), 2477–2493, doi:10.1002/hyp.13742, 2020.

Christopher, S. F., Mitchell, M. J., McHale, M. R., Boyer, E. W., Burns, D. A. and Kendall, C.: Factors controlling nitrogen release from two forested catchments with contrasting hydrochemical responses, Hydrol. Process., 22(1), 46–62, doi:https://doi.org/10.1002/hyp.6632, 2008.

Creed, I. F., Band, L. E., Foster, N. W., Morrison, I. K., Nicolson, J. A., Semkin, R. S. and Jeffries, D. S.: Regulation of nitrate-N release from temperate forests: A test of the N flushing hypothesis, Water Resour. Res., 32(11), 3337–3354, doi:10.1029/96WR02399, 1996.

Durka, W., Schulze, E., Gebauer, G. and Voerkeliust, S.: Effects of forest decline on uptake and leaching of deposited nitrate determined from ^{15}N and ^{18}O measurements, Nature, 372, 765−767, doi: https://doi.org/10.1038/372765a0, 1994.

EANET: Data Report 2010, Network center for EANET (Acid Deposition Monitoring Network in East Asia), Nigata, Japan, 2011.

EANET: Data Report 2011, Network center for EANET (Acid Deposition Monitoring Network in East Asia), Nigata, Japan, 2012.

Fang, Y., Koba, K., Makabe, A., Takahashi, C., Zhu, W., Hayashi, T., Hokari, A. A., Urakawa, R., Bai, E., Houlton, B. Z., Xi, D., Zhang, S., Matsushita, K., Tu, Y., Liu, D., Zhu, F., Wang, Z., Zhou, G., Chen, D., Makita, T., Toda, H., Liu, X., Chen, Q., Zhang, D., Li, Y. and Yoh, M.: Microbial denitrification dominates nitrate losses from forest ecosystems, Proc. Natl. Acad. Sci. U. S. A., 112(5), 1470–1474, doi:10.1073/pnas.1416776112, 2015.

Galloway, J. N., Aber, J. D., Erisman, J. W., Seitzinger, S. P., Howarth, R. W., Cowling, E. B. and Cosby, B. J.: The nitrogen cascade, Bioscience, 53(4), 341–356, doi:10.1641/0006-3568(2003)053[0341:TNC]2.0.CO;2, 2003.

Hattori, S., Nuñez Palma, Y., Itoh, Y., Kawasaki, M., Fujihara, Y., Takase, K. and Yoshida, N.: Isotopic evidence for seasonality of microbial internal nitrogen cycles in a temperate forested catchment with heavy snowfall, Sci. Total Environ., 690, 290–299, doi:10.1016/j.scitotenv.2019.06.507, 2019.

Hirota, A., Tsunogai, U., Komatsu, D. D. and Nakagawa, F.: Simultaneous determination of $\delta^{15}N$ and $\delta^{18}O$ of N_2O and $\delta^{13}C$ of CH_4 in nanomolar quantities from a single water sample, Rapid Commun. Mass Spectrom., 24, 1085–1092, doi:10.1002/rcm.4483, 2010.

Hornberger, G. M., Bencala, K. E. and McKnight, D. M.: Hydrological controls on dissolved organic carbon during snowmelt in the Snake River near Montezuma,

752 Colorado, Biogeochemistry, 25(3), 147–165, doi:10.1007/BF00024390, 1994.
753 Huang, S., Wang, F., Elliott, E. M., Zhu, F., Zhu, W., Koba, K., Yu, Z., Hobbie, E.
754 A., Michalski, G., Kang, R., Wang, A., Zhu, J., Fu, S. and Fang, Y.: Multiyear
755 Measurements on $\Delta^{17}O$ of Stream Nitrate Indicate High Nitrate Production in a
756 Temperate Forest, Environ. Sci. Technol., 54(7), 4231–4239,
757 doi:10.1021/acs.est.9b07839, 2020.
758 Inamdar, S. P. and Mitchell, M. J.: Hydrologic and topographic controls on storm-
759 event exports of dissolved organic carbon (BOC) and nitrate across catchment scales,
760 Water Resour. Res., 42(3), 1–16, doi:10.1029/2005WR004212, 2006.
761 Inoue, T., Nakagawa, F., Shibata, H. and Tsunogai, U.: Vertical Changes in the Flux
762 of Atmospheric Nitrate From a Forest Canopy to the Surface Soil Based on $\Delta^{17}O$
763 Values, J. Geophys. Res. Biogeosciences, 126(4), 1–18, doi:10.1029/2020JG005876,
764 2021.
765 Kaiser, J., Hastings, M. G., Houlton, B. Z., Röckmann, T. and Sigman, D. M.: Triple
766 oxygen isotope analysis of nitrate using the denitrifier method and thermal
767 decomposition of N_2O, Anal. Chem., 79(2), 599–607, doi:10.1021/ac061022s, 2007.
768 Kamisako, M., Sase, H., Matsui, T., Suzuki, H., Takahashi, A., Oida, T., Nakata, M.,
769 Totsuka, T. and Ueda, H.: Seasonal and annual fluxes of inorganic constituents in a
770 small catchment of a Japanese cedar forest near the sea of Japan, Water. Air. Soil
771 Pollut., 195(1–4), 51–61, doi:10.1007/s11270-008-9726-8, 2008.
772 Keeling, D.: The concentration and isotopic abundances of atmospheric carbon

773 dioxide in rural areas, Geochim. Cosmochim. Acta, 13, 322–334,
774 doi:https://doi.org/10.1016/0016-7037(58)90033-4, 1958.
775 Kendall, C., Elliott, E. M. and Wankel, S. D.: Tracing Anthropogenic Inputs of
776 Nitrogen to Ecosystems, Stable Isot. Ecol. Environ. Sci. Second Ed., 375–449,
777 doi:10.1002/9780470691854.ch12, 2008.
778 Kotlash, A. R. and Chessman, B. C.: Effects of water sample preservation and storage
779 on nitrogen and phosphorus determinations: Implications for the use of automated
780 sampling equipment, Water Res., 32(12), 3731–3737, doi:10.1016/S0043-
781 1354(98)00145-6, 1998.
782 Komatsu, D. D., Ishimura, T., Nakagawa, F. and Tsunogai, U.: Determination of the
783 $^{15}N/^{14}N$, $^{17}O/^{16}O$, and $^{18}O/^{16}O$ ratios of nitrous oxide by using continuous-flow
784 isotope-ratio mass spectrometry Daisuke, Rapid Commun. Mass Spectrom., 22, 1587–
785 1596, doi:10.1002/rcm.3493, 2008.
786 Konno, U., Tsunogai, U., Komatsu, D. D., Daita, S., Nakagawa, F., Tsuda, A.,
787 Matsui, T., Eum, Y. J. and Suzuki, K.: Determination of total N2 fixation rates in the
788 ocean taking into account both the particulate and filtrate fractions, Biogeosciences,
789 7(8), 2369–2377, doi:10.5194/bg-7-2369-2010, 2010.
790 McHale, M. R., McDonnell, J. J., Mitchell, M. J. and Cirmo, C. P.: A field-based
791 study of soil water and groundwater nitrate release in an Adirondack forested
792 watershed, Water Resour. Res., 38(4), 2-1-2–16, doi:10.1029/2000wr000102, 2002.
793 McIlvin, M. R. and Altabet, M. A.: Chemical conversion of nitrate and nitrite to

794 nitrous oxide for nitrogen and oxygen isotopic analysis in freshwater and seawater,
795 Anal. Chem., 77(17), 5589–5595, doi:10.1021/ac050528s, 2005.
796 Michalski, G., Scott, Z., Kabiling, M. and Thiemens, M. H.: First measurements and
797 modeling of $\Delta^{17}O$ in atmospheric nitrate, Geophys. Res. Lett., 30(16), 3–6,
798 doi:10.1029/2003GL017015, 2003.
799 Michalski, G., Meixner, T., Fenn, M., Hernandez, L., Sirulnik, A., Allen, E. and
800 Thiemens, M.: Tracing Atmospheric Nitrate Deposition in a Complex Semiarid
801 Ecosystem Using $\Delta^{17}O$, Environ. Sci. Technol., 38(7), 2175–2181,
802 doi:10.1021/es034980+, 2004.
803 Mitchell, M. J., Iwatsubo, G., Ohrui, K. and Nakagawa, Y.: Nitrogen saturation in
804 Japanese forests: An evaluation, For. Ecol. Manage., 97(1), 39–51,
805 doi:10.1016/S0378-1127(97)00047-9, 1997.
806 Morin, S., Sander, R. and Savarino, J.: Simulation of the diurnal variations of the
807 oxygen isotope anomaly ($\Delta^{17}O$) of reactive atmospheric species, Atmos. Chem. Phys.,
808 11(8), 3653–3671, doi:10.5194/acp-11-3653-2011, 2011.
809 Nakagawa, F., Suzuki, A., Daita, S., Ohyama, T., Komatsu, D. D. and Tsunogai, U.:
810 Tracing atmospheric nitrate in groundwater using triple oxygen isotopes: Evaluation
811 based on bottled drinking water, Biogeosciences, 10(6), 3547–3558, doi:10.5194/bg-
812 10-3547-2013, 2013.
813 Nakagawa, F., Tsunogai, U., Obata, Y., Ando, K., Yamashita, N., Saito, T.,
814 Uchiyama, S., Morohashi, M. and Sase, H.: Export flux of unprocessed atmospheric

nitrate from temperate forested catchments: A possible new index for nitrogen saturation, Biogeosciences, 15(22), 7025–7042, doi:10.5194/bg-15-7025-2018, 2018.

Nelson, D. M., Tsunogai, U., Ding, D., Ohyama, T., Komatsu, D. D., Nakagawa, F., Noguchi, I. and Yamaguchi, T.: Triple oxygen isotopes indicate urbanization affects sources of nitrate in wet and dry atmospheric deposition, Atmos. Chem. Phys., 18(9), 6381–6392, doi:10.5194/acp-18-6381-2018, 2018.

Ocampo, C. J., Sivapalan, M. and Oldham, C.: Hydrological connectivity of upland-riparian zones in agricultural catchments: Implications for runoff generation and nitrate transport, J. Hydrol., 331(3–4), 643–658, doi:10.1016/j.jhydrol.2006.06.010, 2006.

Ohte, N., Sebestyen, S. D., Shanley, J. B., Doctor, D. H., Kendall, C., Wankel, S. D. and Boyer, E. W.: Tracing sources of nitrate in snowmelt runoff using a high-resolution isotopic technique, Geophys. Res. Lett., 31(21), 2–5, doi:10.1029/2004GL020908, 2004.

Ohte, N., Tayasu, I., Kohzu, A., Yoshimizu, C., Osaka, K., Makabe, A., Koba, K., Yoshida, N. and Nagata, T.: Spatial distribution of nitrate sources of rivers in the lake Biwa Watershed, Japan: Controlling factors revealed by nitrogen and oxygen isotope values, Water Resour. Res., 46(7), 1–16, doi:10.1029/2009WR007871, 2010.

Paerl, H. W. and Huisman, J.: Climate change: A catalyst for global expansion of harmful cyanobacterial blooms, Environ. Microbiol. Rep., 1(1), 27–37, doi:10.1111/j.1758-2229.2008.00004.x, 2009.

836 Pellerin, B. A., Saraceno, J. F., Shanley, J. B., Sebestyen, S. D., Aiken, G. R.,
837 Wollheim, W. M. and Bergamaschi, B. A.: Taking the pulse of snowmelt: In situ
838 sensors reveal seasonal, event and diurnal patterns of nitrate and dissolved organic
839 matter variability in an upland forest stream, Biogeochemistry, 108(1–3), 183–198,
840 doi:10.1007/s10533-011-9589-8, 2012.
841 Peterjohn, W. T., Adams, M. B. and Gilliam, F. S.: Symptoms of nitrogen saturation
842 in two central Appalachian hardwood forest ecosystems, Biogeochemistry, 35(3),
843 507–522, doi:10.1007/BF02183038, 1996.
844 Piatek, K. B., Mitchell, M. J., Silva, S. R. and Kendall, C.: Sources of nitrate in
845 snowmelt discharge: Evidence from water chemistry and stable isotopes of nitrate,
846 Water. Air. Soil Pollut., 165(1–4), 13–35, doi:10.1007/s11270-005-4641-8, 2005.
847 Riha, K. M., Michalski, G., Gallo, E. L., Lohse, K. A., Brooks, P. D. and Meixner, T.:
848 High Atmospheric Nitrate Inputs and Nitrogen Turnover in Semi-arid Urban
849 Catchments, Ecosystems, 17(8), 1309–1325, doi:10.1007/s10021-014-9797-x, 2014.
850 Rose, L. A., Elliott, E. M. and Adams, M. B.: Triple Nitrate Isotopes Indicate
851 Differing Nitrate Source Contributions to Streams Across a Nitrogen Saturation
852 Gradient, Ecosystems, 18(7), 1209–1223, doi:10.1007/s10021-015-9891-8, 2015.
853 Sabo, R. D., Nelson, D. M. and Eshleman, K. N.: Episodic, seasonal, and annual
854 export of atmospheric and microbial nitrate from a temperate forest, Geophys. Res.
855 Lett., 43(2), 683–691, doi:10.1002/2015GL066758, 2016.
856 Sase, H., Takahashi, A., Sato, M., Kobayashi, H., Nakata, M. and Totsuka, T.:

857 Seasonal variation in the atmospheric deposition of inorganic constituents and canopy
858 interactions in a Japanese cedar forest, Environ. Pollut., 152(1), 1–10,
859 doi:10.1016/j.envpol.2007.06.023, 2008.
860 Sase, H., Saito, T., Takahashi, M., Morohashi, M., Yamashita, N., Inomata, Y.,
861 Ohizumi, T. and Nakata, M.: Transboundary air pollution reduction rapidly reflected
862 in stream water chemistry in forested catchment on the Sea of Japan coast in central
863 Japan, Atmos. Environ., 248(November 2020), 118223,
864 doi:10.1016/j.atmosenv.2021.118223, 2021.
865 Sebestyen, S. D., Ross, D. S., Shanley, J. B., Elliott, E. M., Kendall, C., Campbell, J.
866 L., Dail, D. B., Fernandez, I. J., Goodale, C. L., Lawrence, G. B., Lovett, G. M.,
867 McHale, P. J., Mitchell, M. J., Nelson, S. J., Shattuck, M. D., Wickman, T. R.,
868 Barnes, R. T., Bostic, J. T., Buda, A. R., Burns, D. A., Eshleman, K. N., Finlay, J. C.,
869 Nelson, D. M., Ohte, N., Pardo, L. H., Rose, L. A., Sabo, R. D., Schiff, S. L.,
870 Spoelstra, J. and Williard, K. W. J.: Unprocessed Atmospheric Nitrate in Waters of
871 the Northern Forest Region in the U.S. and Canada, Environ. Sci. Technol., 53(7),
872 3620–3633, doi:10.1021/acs.est.9b01276, 2019.
873 Stoddard, J. L.: Long-Term Changes in Watershed Retention of Nitrogen, , 223–284,
874 doi:10.1021/ba-1994-0237.ch008, 1994.
875 Tsunogai, U., Komatsu, D. D., Daita, S., Kazemi, G. A., Nakagawa, F., Noguchi, I.
876 and Zhang, J.: Tracing the fate of atmospheric nitrate deposited onto a forest
877 ecosystem in Eastern Asia using $\Delta^{17}O$, Atmos. Chem. Phys., 10(4), 1809–1820,

878 doi:10.5194/acp-10-1809-2010, 2010.
879 Tsunogai, U., Daita, S., Komatsu, D. D., Nakagawa, F. and Tanaka, A.: Quantifying
880 nitrate dynamics in an oligotrophic lake using $\Delta^{17}O$, Biogeosciences, 8(3), 687–702,
881 doi:10.5194/bg-8-687-2011, 2011.
882 Tsunogai, U., Komatsu, D. D., Ohyama, T., Suzuki, A., Nakagawa, F., Noguchi, I.,
883 Takagi, K. and Nomura, M.: Quantifying the effects of clear-cutting and strip-cutting
884 on nitrate dynamics in a forested watershed using triple oxygen isotopes as tracers, ,
885 (1), 5411–5424, doi:10.5194/bg-11-5411-2014, 2014.
886 Tsunogai, U., Miyauchi, T., Ohyama, T., Komatsu, D. D., Nakagawa, F., Obata, Y.,
887 Sato, K. and Ohizumi, T.: Accurate and precise quantification of atmospheric nitrate
888 in streams draining land of various uses by using triple oxygen isotopes as tracers,
889 Biogeosciences, 13(11), 3441–3459, doi:10.5194/bg-13-3441-2016, 2016.
890 Tsunogai, U., Miyauchi, T., Ohyama, T., Komatsu, D. D., Ito, M. and Nakagawa, F.:
891 Quantifying nitrate dynamics in a mesotrophic lake using triple oxygen isotopes as
892 tracers, Limnol. Oceanogr., 63, S458–S476, doi:10.1002/lno.10775, 2018.
893 Vitousek, P. M. and Howarth, R. W.: Nitrogen limitation on land and in the sea: How
894 can it occur?, Biogeochemistry, 13(2), 87–115, doi:10.1007/BF00002772, 1991.
895 Yamazaki, A., Watanabe, T. and Tsunogai, U.: Nitrogen isotopes of organic nitrogen
896 in reef coral skeletons as a proxy of tropical nutrient dynamics, Geophys. Res. Lett.,
897 38(19), 1–5, doi:10.1029/2011GL049053, 2011.